WIND PROFILING BY PASSIVE OPTICAL METHOD

Vadim Dudorov, Anna Eremina

V.E. Zuev Institute of Atmospheric Optics, Rus. Acad. Sci., Tomsk 634021, Russia

ABSTRACT

Possibilities of the wind speed profiling along an observation path of a distant object from the analysis of a video sequence of images of the object are studied in this work. The method is based on the analysis of two neighbor frames of a video sequence of incoherent images. The wind velocity retrieved is compared with data of acoustic anemometers.

1. INTRODUCTION

There are several optical approaches to the remote measurements of crosswind speed [1-6]. An evident advantage of passive techniques is that they do not need in proper radiation sources. This allows measurement instruments to be simplified and their cost to be reduced, as well as the domain of applicability of contactless wind speed meters to be expanded to the situations where it is impossible to mount a radiation transmitter/receiver at one of the ends of an atmospheric path under study, e.g., in problems of line-of-sight correction.

We suggest an approach which is based on the analysis of the dynamics of anisoplanar (inhomogeneous) turbulent distortions in object images formed by wide-field cameras [7–10]. In this case, the shift of distortions in an object image, which characterizes the speed of displacement of turbulent inhomogeneities, can be determined from the analysis of two neighbor frames of a video sequence of images. The advantages of this approach are a high speed due to the lack of a need in accumulation of a series of observations to construct temporal correlation functions and a capability of determining the instantaneous wind speed.

Two key problems are to be solved for the development of the method for wind profiling: first, it is necessary to derive a relationship between turbulent inhomogeneities and image distortions caused by them, and, second, it is required to identify (visualize) turbulent distortions in images of distant objects.

2. INFLUENCE OF LOCATION OF TURBULENT INHOMOGENEITIES ON THE CHARACTER OF DISTORTIONS CAUSED BY THEM

To determine the relation between the character of distortions in the image of an object and the location of atmospheric inhomogeneities in the region between the object and an observer, the process of imaging in the presence of some bounded region (thin layer) of turbulent inhomogeneities along the observation path was numerically simulated. To suppress the effect of the structure of complex objects, we choose a test object with the rough (Lambertian) surface and periodic variations in the reflection coefficient like

$$T(\mathbf{r}) = \exp\left\{-\left[1+\sin\left(x/b\right)\right]^{10}\right\}, \qquad (1)$$

Figure 1 shows the scheme of formation of the incoherent image of an object in the presence of a thin layer of turbulent inhomogeneities (one phase screen) located at a different distance from the observer z_{ts}. In this case, the displacement of the phase screen along the optical axis allows us to separate the effect of air inhomogeneities located at different distances from the receiving system along the observation path.

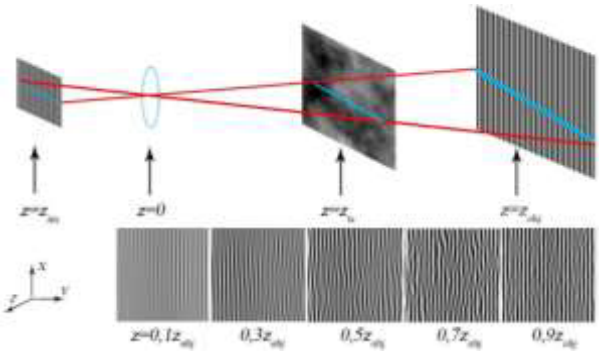

Fig.1. Scheme of formation of an incoherent image of an object in the presence of a thin layer of turbulent inhomogeneities (single phase screen).

The numerical simulation results allowed us to ascertain that the characteristic size of anisoplanar distortions produced by the layer of a turbulent medium (phase screen) located at the distance z_{ts} from the observer inversely relates to the distance:

$$a_{anisopl}(z_{ts}) = \frac{A}{z_{ts} / z_{obj}}, \qquad (2)$$

where A is the dimensional parameter and is a function of the atmospheric conditions and receiving system.

3. TURBULENT INHOMOGENEITIES VISUALISATION

During the processing of images analyzed, the information about the object structure is to be filtered, i.e., the so-called quality map of an image should be constructed, which includes only data on atmospheric distortions. Based on the sharpness functional, the image quality map can be defined in the form:

$$Q(\mathbf{r}, a_k, t) = \left|\nabla_{\mathbf{r}} I(\mathbf{r}, t)\right|^2 \otimes K(\mathbf{r}, a_k), \qquad (2)$$

where $\nabla_{\mathbf{r}} = \vec{i}\frac{\partial}{\partial x} + \vec{j}\frac{\partial}{\partial y}$ is the gradient vector, $\left|\nabla_{\mathbf{r}} I(\mathbf{r}, t)\right|^2$ is the image sharpness functional; a_k is the smoothing coefficient; $K(\mathbf{r}, a_k)$ is the certain smoothing function defined as Gaussian:

$$K(\mathbf{r}, a_k) = \frac{1}{\pi a_k^2} \exp\left(-r^2 / a_k^2\right) \qquad (3)$$

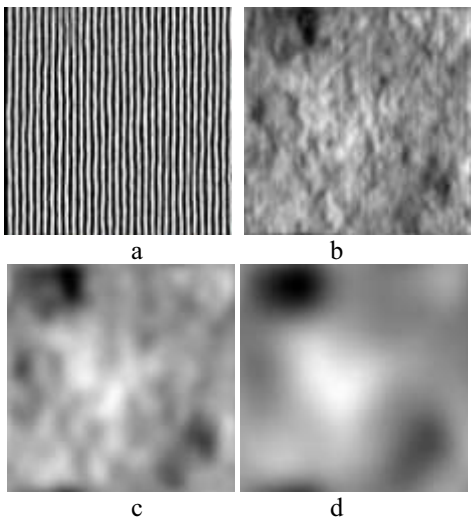

Fig.2. (a) Object image and its quality map in a turbulent medium at different values of the smoothing coefficient: (b) a_k=0.7a_t, (c) 2.5a_t, and (d) 6.0a_t. The distance to the object $z_{obj} = 0.1ka_t^2$; b=0.2a_t; N_z=5; R_{obj}=40a_t; N_R=512; the ratio of the receiving aperture diameter to the Fried length $2a_t/r_0 = 4$.

Figure 2 shows an object and the quality maps for different values of the smoothing coefficient a_k. It is seen that the characteristic size of distortions $a_{anisopl}$ can be controlled by variations in a_k when analyzing the dynamics of the distortions in the video sequence of images of the object under study with the aim of distinguishing air regions at different distances from the recording equipment.

4. WIND PROFILING METHOD

To profile the wind speed in an arbitrary section of the atmosphere, the observation path between the object and receiving optical system is divided into N segments; the contribution of every segment is considered similar to the contribution of an infinitely thin screen. The algorithm for wind speed profiling at the object observation path is the following:

- the number N of layers of turbulent inhomogeneities, for which the drift velocity is to be calculated, is determined;

- the smoothing parameters $a_{filtr}^{(i)} = \frac{A}{z_{ts}^{(i)} / z_{obj}}$ are calculated for each ith inhomogeneous layer centered in the plane $z_{ts}^{(i)}$,

- the image quality map $Q(\mathbf{r}, a_{\min}, t) = \nabla_{\mathbf{r}}^2 I(\mathbf{r}, t) \otimes K(\mathbf{r}, a_{\min})$ is calculated, which allows filtering only the object structure and remaining the information about distortions. The convolution kernel can be defined as $K(\mathbf{r}, a) = \exp\left(-r^2 / a^2\right)$;

- the function $Q(\mathbf{r}, a_{filtr}^{(1)}, t) = \nabla_{\mathbf{r}}^2 I(\mathbf{r}, t) \otimes K(\mathbf{r}, a_{filtr}^{(1)})$ is calculated, which provides for filtering small-scale inhomogeneities introduced by turbulent inhomogeneities located farther than the first layer;

- the drift velocity of the first layer $\mathbf{V}_1$ is calculated by the equation $\mathbf{V}_i(t) = \frac{\Delta\mathbf{r}(t)}{\Delta t} \cdot \frac{z_i}{z_{im}}$, where $\Delta\mathbf{r}(t) = \arg\max\left[R(\mathbf{r}, t)\right]$,

$R(\mathbf{r},t) = Q(\mathbf{r}, a_{filtr}^{(i)}, t) \otimes Q(-\mathbf{r}, a_{filtr}^{(i)}, t + \Delta t)$ is the correlation function of the image quality maps at different time points;

- the difference $\Delta Q^{(1)}(\mathbf{r},t) = Q(\mathbf{r}, a_{\min}, t) - Q(\mathbf{r}, a_{filtr}^{(1)}, t)$ is calculated, which allows filtering distortions introduced by the first layer of turbulent inhomogeneities;

- the function $Q(\mathbf{r}, a_{filtr}^{(2)}, t) = \Delta Q^{(1)}(\mathbf{r},t) \otimes K(\mathbf{r}, a_{filtr}^{(2)})$ is calculated to filter the small-scale distortions introduced by turbulent inhomogeneities located farther than the second layer;

- the drift velocity of the second layer $\mathbf{V}_2$ is calculated;

- the difference $\Delta Q^{(2)}(\mathbf{r},t) = \Delta Q^{(1)}(\mathbf{r},t) - Q(\mathbf{r}, a_{filtr}^{(2)}, t)$ is calculated;

- the last steps are repeated until $\mathbf{V}_N$ is calculated.

This algorithm allows serial filtration of distortions introduces by each layer of turbulent inhomogeneities (phase screen), beginning from the layer the closest to the observer toward the object. It should be noted that there are inhomogeneities on different scales in each turbulent layer. It is evident that imaging through a real atmosphere can be subjected to distortions on a certain scale induced by air inhomogeneities located at different distances from the observer. In this case, when using the method suggested, distortions introduced by different turbulent layers are filtered only partially.

For more rigorous filtration of the distortions of near turbulent layers, an additional parameter can be used, i.e., the angular size of the image region to be analyzed. We suggest reducing this region to sizes of about the characteristic size of the distortions which are to be filtered. This reduction also allows the spatial averaging of the measured drift velocity of distortions over the whole area of the object observed and, thus, a decrease in the random error of wind speed calculated along the observation path.

5. COMPARISON OF THE RESULTS OF PROCESSING OF VIDEO SEQUENCE WITH CONTACT MEASUREMENTS OF WIND VELOCITY

The efficiency of the method suggested was estimated during processing of a video image of a real object. Shooting was conducted with a frequency of 100 Hz. The accuracy of wind speed retrieval by a passive optical method is determined from the comparison with measurements of ten acoustic anemometers, equispaced along a 500-m atmospheric path. Figure 3 shows the object image and its sharpness functional. The upper part of the image (a fragment of deciduous forest) was used during the processing.

The wind velocity strongly changed along the observation path during imaging. Therefore, to weakens the effect of the random measurement error, the path was divided into three segments, within which the wind velocity value averaged over three (or four) anemometers was found.

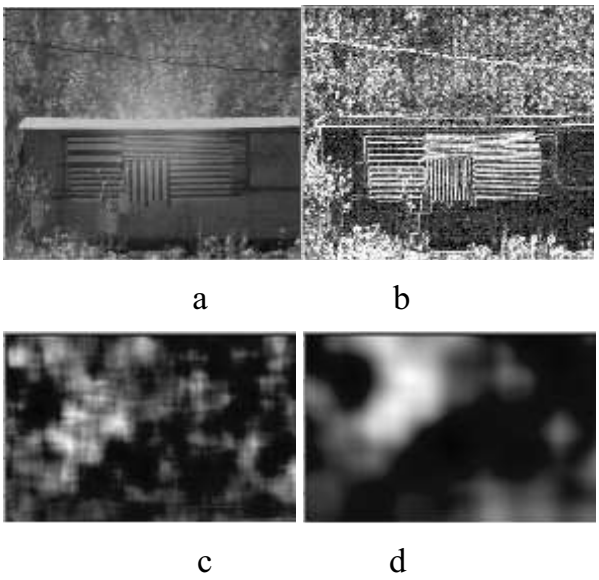

Fig. 3. Object image (a), its sharpness functional (b) and quality maps (c-d). The horizontal size of the region observed is 5 m; a_f=5 cm, the distance z_{obj} =500 m, and Δt = 10 ms.

Figure 4 shows that the wind speed retrieved in the nearby layers of turbulent inhomogeneities is in a good agreement with the wind speed contact measurements averaged over three acoustic anemometers.

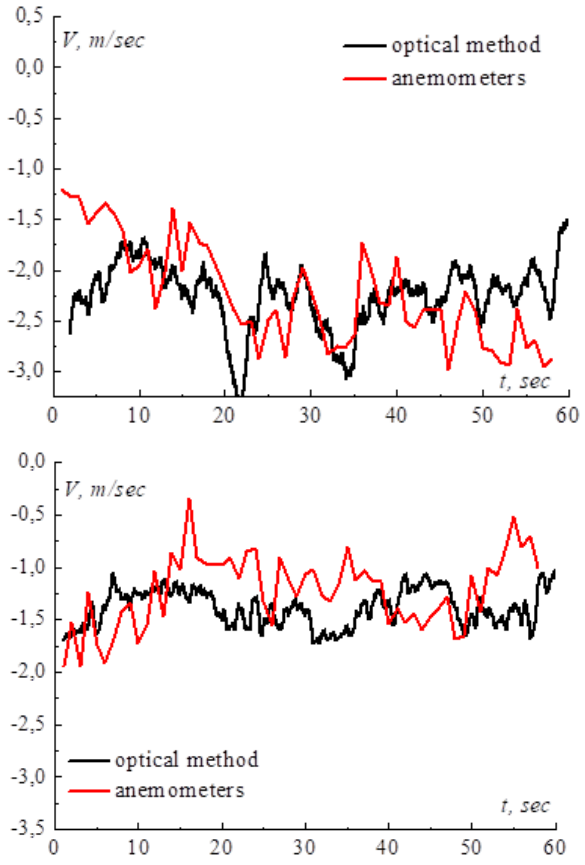

Fig. 4. Dynamics of the (a) retrieved wind speed near the observer (black curve) and (b) wind speed averaged over the central path segment in comparison with contact measurements by 10 acoustic anemometers equispaced along the path (red curve).

4. CONCLUSIONS

The comparison of the results of the algorithm developed by us showed a good agreement with contact measurements. The wind velocity is retrieved with the minimal error near the receiving optical system. Retrieval of wind speed in the atmospheric region near the object is problematic due to the small scale of the distortions introduced by it. To increase the range of crosswind determination by the method suggested, it is necessary to increase the camera resolution.

ACKNOWLEDGEMENTS

The work was supported by the Russian Science Foundation (project No. 18-79-00179).

REFERENCES

[1] Holmes, R.B., “Passive optical wind profilometer,”. US patent USO05469250A, (1995).
[2] Belenkii M., “Passive crosswind profiler.” US patent 0128136 A1, (2010).
[3] Lukin, V. P., Lavrinov, V. V., Botugina, N. N.,Emaleev, O. N. and Nosov, V. V., "Differential turbulence and wind velocity meters," Proc. SPIE 6733, 67330N (2007)
[4] Banakh, V. A. and Marakasov, D. A., “Wind velocity profile reconstruction from intensity fluctuations of a plane wave propagating in a turbulent atmosphere,” Opt. Lett. 32(15), 2236–2238 (2007).
[5] Varshneya, D., Griggs, S. and Jeffers, L., “Electro-optic system for crosswind measurement,” US patent US9157701B2, (2013).
[6] Porat, O., Shapira, J., “Crosswind sensing from optical-turbulence-induced fluctuations measured by a video camera,” Appl. Opt. 49(28), 5236-5244 (2010).
[7] Dudorov, V. V., Eremina, A. S., “Determination of atmospheric turbulent inhomogeneity wind drift from sequence of incoherent images,” Proc. SPIE 9292, 92921F (2014).
[8] Dudorov, V. V., Eremina A.S., “Filtration of optical image distortions for retrieving the drift velocity of atmospheric turbulence inhomogeneities,” Proc. SPIE 9680, 96802E (2015).
[9] Dudorov, V. V., Eremina A.S., “Possibilities of crosswind profiling based on incoherent imaging,” Proc. SPIE 10035, 100351Q (2016).
[10] Dudorov, V. V., Eremina, A. S., “Retrieval of crosswind velocity based on the analysis of remote object images: Part 1 — drift of a thin layer of turbulent inhomogeneities,” Atmospheric and Oceanic Optics 30(5), 422-428 (2017).
[11] Dudorov, V. V., Eremina, A. S., “Retrieval of crosswind velocity based on the analysis of remote object images: Part 2—Drift of turbulent,” Atmospheric and Oceanic Optics 30(6), 596-603 (2017).
[12] Dudorov, V. V., Eremina A.S., “Visualization of the wind drift of turbulent inhomogeneities,” Proc. SPIE 10787, 1078708-1-9 (2018).